

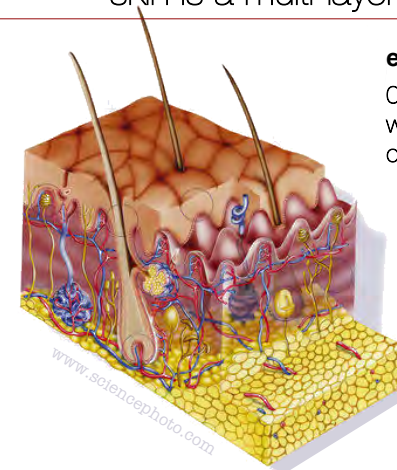
11 - volume growth skin expansion & growth



11 - volume growth - skin expansion

1

skin is a multi-layered material



epidermis

0.06-1.0mm thick
waterproof, protective
outer layer

dermis

1.0-3.0mm thick
load bearing
inner layer

hypodermis

fatty layer
attaching skin
to bone and muscle

motivation - skin growth

2



skin expansion

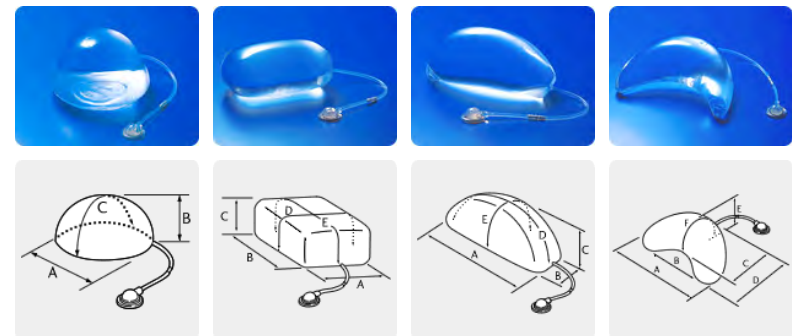
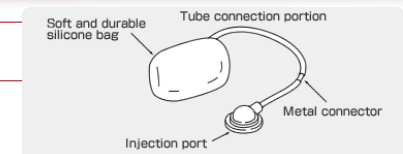
skin expansion is a technique used by plastic and restorative surgeons to cause the body grow additional skin. keeping living tissues under tension causes new cells to form and the amount of tissue to increase. in some cases, this may be accomplished by the implantation of inflatable balloons under the skin. by far the most common method, the surgeon inserts the inflatable expander beneath the skin and periodically, over weeks or months, injects a saline solution to slowly stretch the overlying skin. the growth of tissue is permanent, but will retract to some degree when the expander is removed. within the past 30 years, skin expansion has revolutionized reconstructive surgery. typical applications are breast reconstruction, burn injuries, and pediatric plastic surgery.



motivation - skin growth

3

skin expanders

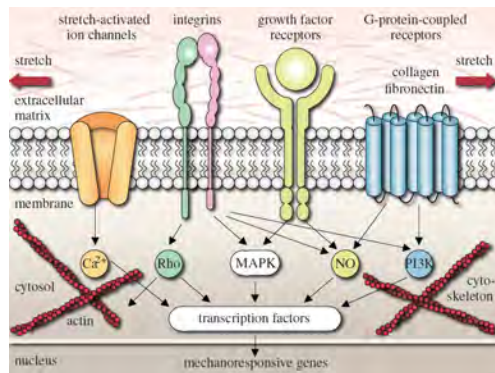


copyright © 2005 koken co., ltd.

motivation - skin growth

4

mechanotransduction of growing skin



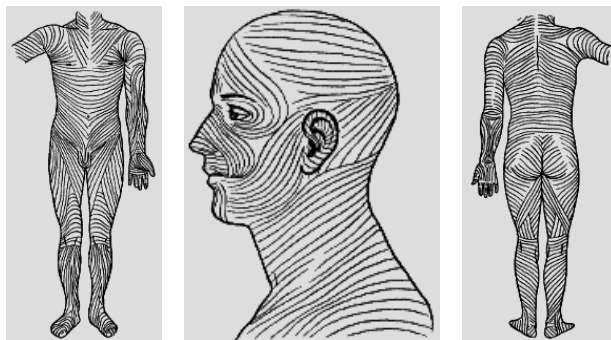
transmembrane mechanosensors in the form of stretch-activated ion channels, integrins, growth factor receptors, and G-protein-coupled receptors translate extracellular signals into intracellular events, which activate a cascade of interconnected signaling pathways. biomechanical and biochemical signals converge in the activation of transcription factors, activating gene expression. mechanotransduction triggers increased mitotic activity and increased collagen synthesis, resulting in an increase in skin surface area to restore the homeostatic equilibrium state.

wong et al. [2011], zollner et al. [2011]

motivation - skin growth

5

langer's lines - anisotropy of human skin



lines of tension - orientation of collagen fiber bundles

carl ritter von langer [1819-1887]

constitutive equations of skin

7



langer's lines - anisotropy of human skin

langer's lines, sometimes called cleavage lines, are topological lines drawn on a map of the human body. they are defined by the direction in which the human skin would split when struck with a spike. langer's lines correspond to the natural orientation of collagen fibers in the dermis and epidermis. knowing the direction of langer's lines within a specific area of the skin is important for surgical procedures. particularly cosmetic surgery involving the skin. if a surgeon has a choice about where and in what direction to place an incision, he may choose to cut in the direction of langer's lines. incisions made parallel to langer's lines may heal better and produce less scarring than those cut across.

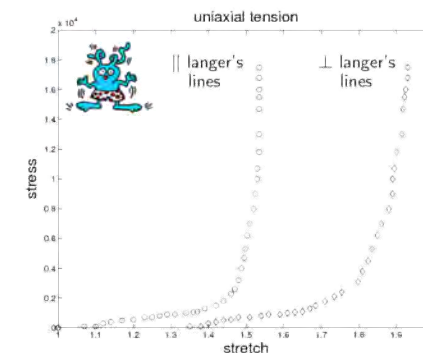


WIKIPEDIA
The Free Encyclopedia

constitutive equations of skin

6

langer's lines - anisotropy of rabbit skin



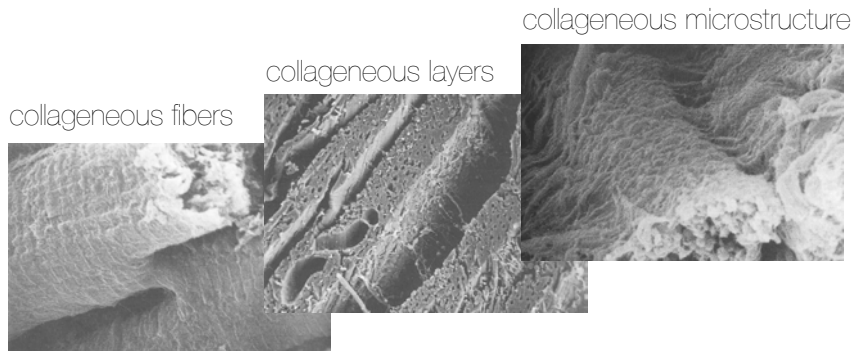
stiffer || to langer's lines - stress locking @crit stretch

lanir & fung [1974]

constitutive equations of skin

8

what is it that makes skin anisotropic? collagen fibers



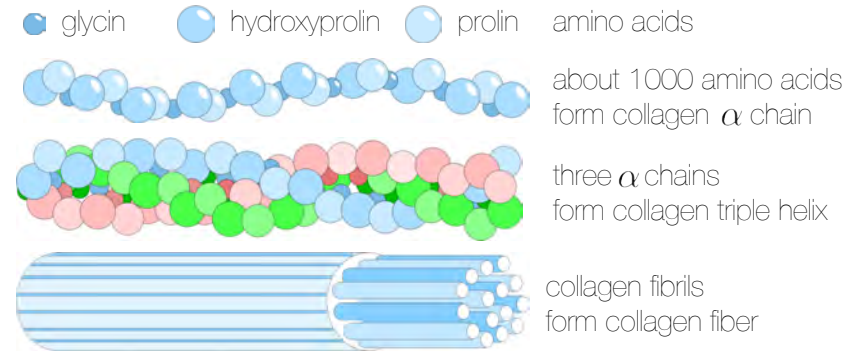
directional strengthening due to collagen fibers

humphrey [2002]

constitutive equations of skin

9

collagen fibers - hierarchical microstructure



directional strengthening due to collagen fibers

constitutive equations of skin

10

statistical mechanics of long chain molecules



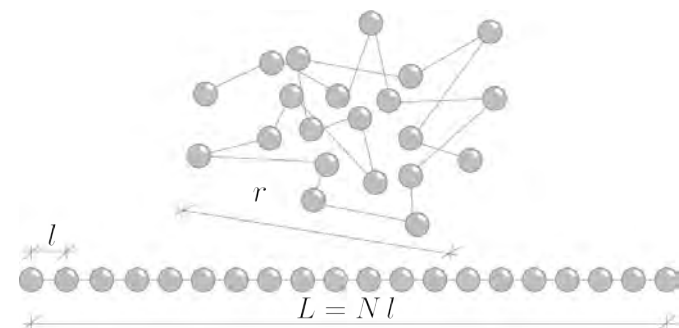
entropic elasticity - entropy increases upon stretching

kuhn [1936], [1938], porod [1949], kratky & porod [1949], treolar [1958], flory [1969], bustamante, smith, marko & siggia [1994], marko & siggia [1995], rief [1997], holzapfel [2000], bischoff, arruda & grosh [2000], [2002], ogden, saccomandi & sgura [2006]

constitutive equations of skin

11

uncorrelated chain model - freely jointed chain



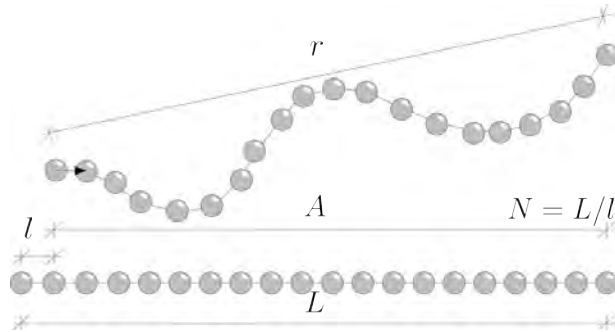
$$\psi^{\text{fjc}} = k \theta N \left[\frac{r}{L} \mathcal{L}^{-1} + \ln \left(\frac{\mathcal{L}^{-1}}{\sinh(\mathcal{L}^{-1})} \right) \right]$$

micromechanically motivated parameter - contour length L

constitutive equations of skin

12

correlated chain model - wormlike chain



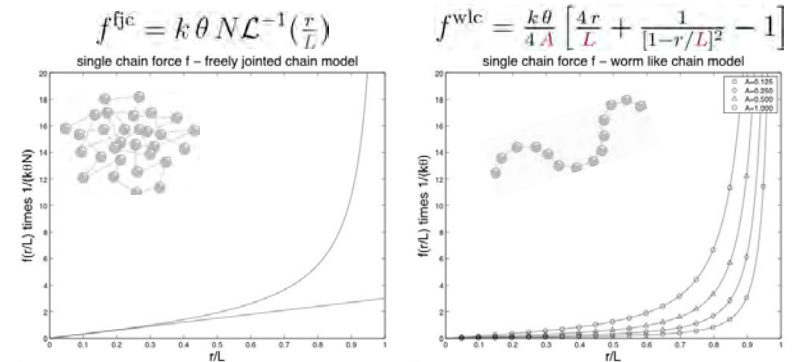
$$\psi^{wlc} = \frac{k\theta L}{4A} \left[2 \frac{r^2}{L^2} + \frac{1}{[1 - r/L]} - \frac{r}{L} \right]$$

micromechanically motivated parameters - contour length L and persistence length A

constitutive equations of skin

13

uncorrelated vs correlated chain model



characteristic locking behavior - initial stiffness of wlc

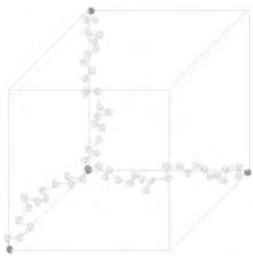
micromechanically motivated parameters - contour length L and persistence length A

constitutive equations of skin

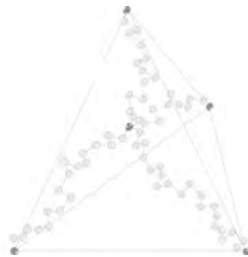
14

chain network models

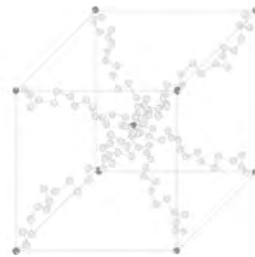
three chain model



four chain model



eight chain model



representative isotropic network of cross-linked chains

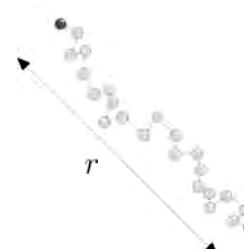
flory & rehner [1943], james & guth [1943], wang & guth [1952], treloar [1958], arruda & boyce [1993], wu & van der giessen [1993], boyce [1996], boyce & arruda [2000], bischoff, arruda & grosh [2002], miehe, göktepe & lulei [2004]

constitutive equations of skin

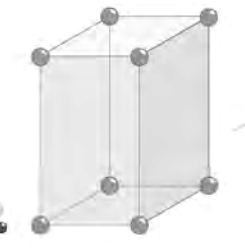
15

generalized eight chain model

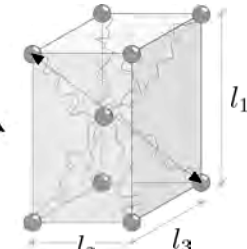
eight single chains



isotropic cell matrix



eight chain model



$$\Psi^{chn} = \frac{1}{8} \gamma^{chn} \sum_{i=1}^8 \psi^{wlc}(r) \quad \text{with} \quad r = r(\mathbf{F})$$

$$\Psi^{iso} = \frac{1}{2} \lambda \ln^2(\det(\mathbf{F})) + \frac{1}{2} \mu [\mathbf{F}^t : \mathbf{F} - n^{\dim} - 2 \ln(\det(\mathbf{F}))]$$

micromechanically motivated parameters - chain density γ^{chn} and cell dimensions l_1, l_2, l_3

constitutive equations of skin

16

generalized eight chain model

- general case **orthotropic** network model

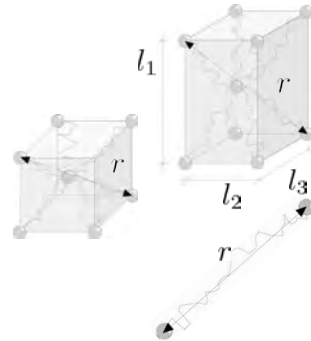
$$l_1 \neq l_2 \neq l_3 \quad r = \sqrt{l_1^2 \bar{I}_1^C}$$

- special case **isotropic** network model

$$l_1 = l_2 = l_3 = l \quad r = l \sqrt{\bar{I}_1^C}$$

- special case **transversely isotropic** model

$$l_2 = l_3 = 0 \quad r = l_1 \sqrt{\bar{I}_1^C}$$



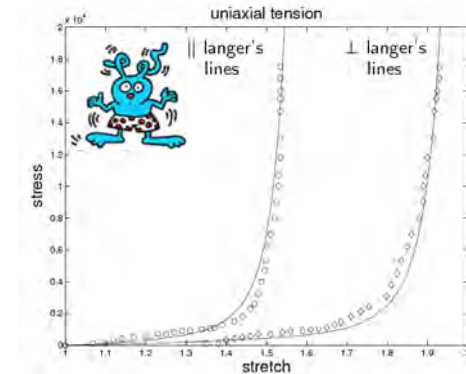
traditional arruda boyce model as special case

$$\text{invariants } \bar{I}_1^C = \mathbf{C} : \mathbf{I} \text{ and } \bar{I}_I^C = \mathbf{n}_I \cdot \mathbf{C} \cdot \mathbf{n}_I$$

constitutive equations of skin

17

experiment vs simulation - rabbit skin



stiffer || to langer's lines - stress locking @crit stretch

lanir & fung [1974], kuhl, garikipati, arruda & grosh [2005]

constitutive equations of skin

18

sometimes skin is damaged...



congenital nevocytic nevi, pigmented surface lesions, are present in one per cent of newborns. one in 20,000 newborns is born with a giant congenital nevus, larger than 10cm in diameter. congenital nevi need to be removed, usually about 6 months after birth, not only because of their cosmetic appearance, but also because of their high potential for malignant change.

motivation - skin growth

19

... but we can repair it

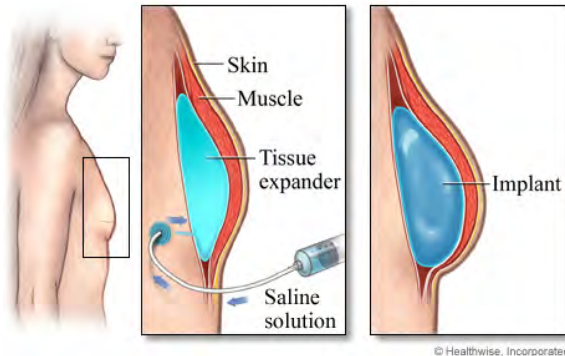


partial reconstruction of right ear. fig 1. preoperative status of partial traumatic amputation of right ear. fig 2. a rubber balloon is inserted in the subcutaneous tissue. fig 3. the rubber balloon is inflated gradually over a period of six weeks. fig 4. upon removal of the balloon, a c-shaped autogenous graft was introduced and covered by a double pedicled tubed flap fashioned from the skin expanded by balloon inflation. neumann [1957]

motivation - skin growth

20

skin expansion and growth - breast reconstruction



within the past 30 years, tissue expansion has revolutionized reconstructive surgery. typical applications are breast reconstruction, burn injuries, and pediatric plastic surgery. natural tissue expansion can be observed in pregnancy, where the local tissue expands and growth in area in response to tension.

motivation - skin growth

21

skin expansion and growth - facial reconstruction



eight-year-old boy who had a nevus removed as an infant. tissue expansion is completed in approximately ten weeks. the use of tissue expansion in cosmetic procedures is often limited by the significant deformity the patient must temporarily accept during the four to six week long procedure. mangubat [2010]

motivation - skin growth

22

skin expansion and growth - facial reconstruction



in this study of reconstruction of the forehead in children, the average number of surgical procedures required to complete reconstruction was six, involving an average of three tissue expansion procedures. gosain & cortes [2007]

motivation - skin growth

23

skin expansion and growth - ear gauging



there are many different methods you can choose from to stretch your ears. always wait at least one month between stretching. failure to stick to this could result in your earlobe puckering, being very thin, or even tearing completely apart. **tapering** is the most common way to stretch ears today. it involves the use of a taper, a rod that is larger at one end, specifically made for this purpose. the taper is lubricated and pushed through the hole until the larger end is flush with the earlobe. rings are then pushed through, parallel to the end of the taper. no equipment is used **dead stretching**. larger jewelry is just forced through the existing piercing. large **weights** can be used to stretch the piercing.



motivation - skin growth

24

skin expansion and growth - lip plates

among the surma and mursi in ethiopia, about 6 to 12 months before marriage the woman's lip is pierced, usually at around the age of 15 to 18. the initial piercing is done as an incision of the lower lip of 1 to 2 cm length, and a simple wooden peg is inserted. after the wound has healed, which usually takes 2 or 3 weeks, the peg is replaced with a slightly bigger one. at a diameter of about 4 cm the first lip plate made of clay is inserted. every woman crafts her plate by herself and takes pride in including some ornamentation. the final diameter ranges from about 8 cm to over 20 cm. the plate's size is a sign of social or economical importance in some tribes.

<http://www.mursi.org>



motivation - skin growth

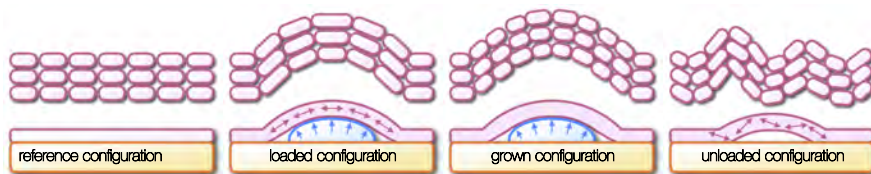
25



motivation - skin growth

26

schematic sequence of tissue expansion

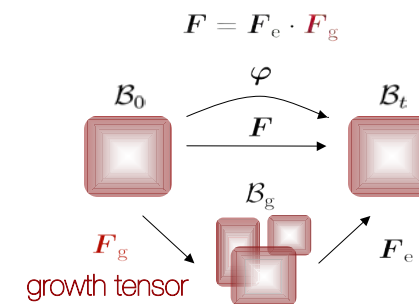


at biological equilibrium, the skin is in a physiological state of resting tension. a tissue expander is implanted subcutaneously between the skin and the hypodermis. when the expander is inflated, mechanical stretch induces cell proliferation causing the skin to grow. growth restores the state of resting tension. expander deflation reveals residual stresses in the skin layer.

kinematic equations

27

kinematics of finite growth



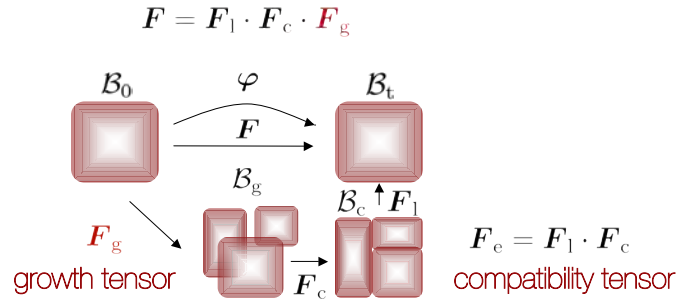
multiplicative decomposition

lee [1969], simo [1992], rodriguez, hoger & mc culloch [1994], epstein & maugin [2000], humphrey [2002], ambrosi & mollica [2002], himpel, kuhl, menzel & steinmann [2005]

kinematic equations

28

kinematics of finite growth



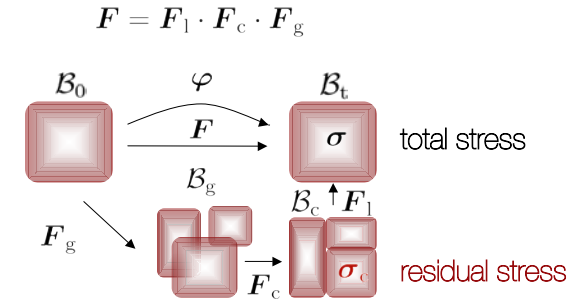
multiplicative decomposition

lee [1969], simo [1992], rodriguez, hoger & mc culloch [1994], epstein & maugin [2000], humphrey [2002], ambrosi & mollica [2002], himpel, kuhl, menzel & steinmann [2005]

kinematic equations

29

kinematics of finite growth



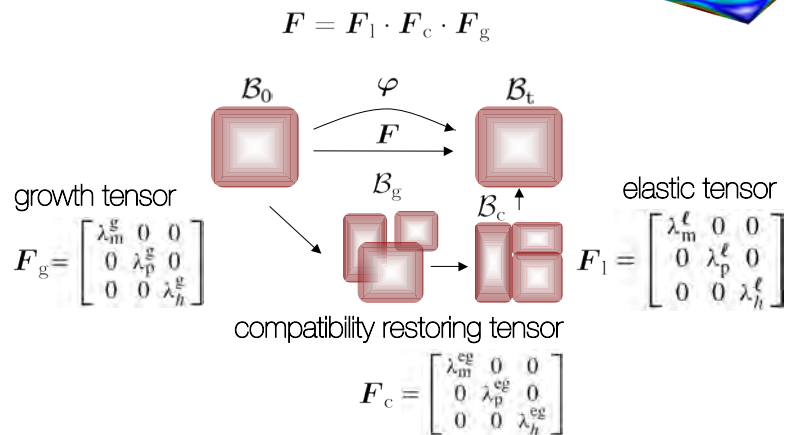
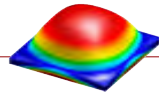
residual stress

the additional deformation of squeezing the grown parts back to a compatible configuration gives rise to residual stresses (see thermal stresses)

kinematic equations

30

skin expansion and growth

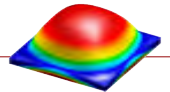


socci, pennati, gervaso, vena [2007]

example - skin expansion

31

skin expansion and growth



- growth law $\dot{\mathbf{F}}^g = \dot{\mathbf{U}}^g = k_\lambda \begin{bmatrix} \lambda_m^\ell - 1 & 0 & 0 \\ 0 & \lambda_p^\ell - 1 & 0 \\ 0 & 0 & 0 \end{bmatrix}$
- increase in mass $\dot{m} = \delta \int_V \text{div}(\mathbf{v}^g) dV = \delta \int_V (D_{11}^g + D_{22}^g + D_{33}^g) dV$
- rate of growth deformation tensor $\mathbf{D}^g = \frac{1}{2} [\dot{\mathbf{U}}^g (\mathbf{U}^g)^{-1} + (\mathbf{U}^g)^{-1} \dot{\mathbf{U}}^g]$
- rate of mass increase $\dot{m} = \delta k_\lambda \int_V \left[\frac{(\lambda_m^l - 1)}{\lambda_m^g} + \frac{(\lambda_p^l - 1)}{\lambda_p^g} \right] dV$

socci, pennati, gervaso, vena [2007]

example - skin expansion

32

skin expansion and growth

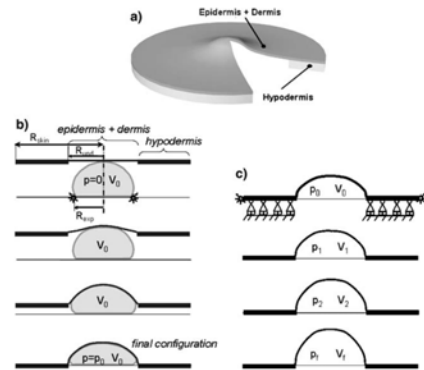


Fig 2. 2a. Sketch of model of expanded skin showing the two considered layers. 2b. First step of simulation of skin expansion: three successive phases of skin-expander interaction. 2c. Second step of simulation of skin expansion: three successive phases of skin-expander model.

socci, pennati, gervaso, vena [2007]

example - skin expansion

33

skin expansion and growth

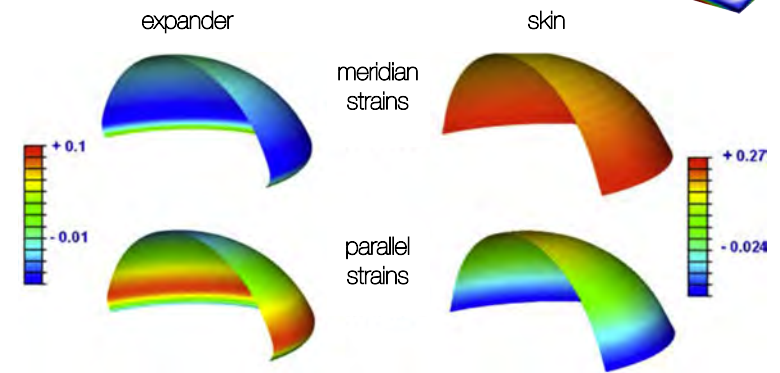


Fig 7. Contour plot of logarithmic principal strains for expander (left) and skin (right) at volume of 550 ml.

socci, pennati, gervaso, vena [2007]

example - skin expansion

34

skin expansion and growth

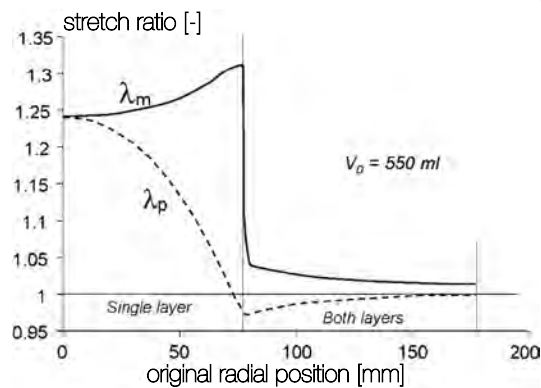


Fig 8. Meridian and parallel stretch ratios vs. distance from the axis of symmetry of the two skin regions (single layer and two layers) after expander injection at reference volume V_0 .

socci, pennati, gervaso, vena [2007]

example - skin expansion

35

skin expansion and growth

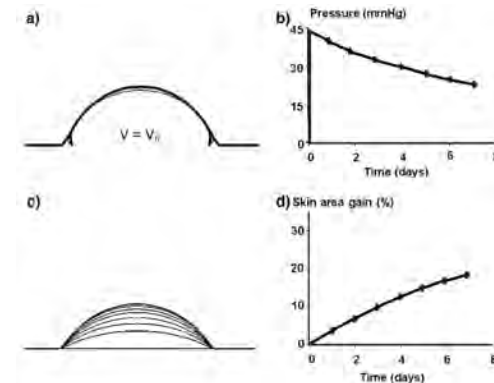


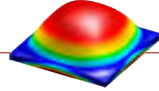
Fig 10. Results of skin growth simulation. 10a. Configurations of expander and expander skin immediately after inflation (thin line) and one week post inflation (thick line). 10b. Pressure decrease during one week after inflation. 10c. Different stress-free configurations at times d0 to d7 at increments of one day. 10d. Percentage of skin area gain.

socci, pennati, gervaso, vena [2007]

example - skin expansion

36

stretch-induced area growth



- deformation gradient

$$\mathbf{F} = \mathbf{F}^e \cdot \mathbf{F}^g \quad \text{with} \quad \mathbf{F} = \nabla_X \boldsymbol{\varphi}$$

- volume change

$$J = J^e J^g \quad \text{with} \quad J = \det(\mathbf{F}) > 0$$

- area change

$$\vartheta = \vartheta^e \vartheta^g \quad \text{with} \quad \vartheta = \|\text{cof}(\mathbf{F}) \cdot \mathbf{n}_0\|$$

- growth tensor

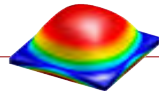
$$\mathbf{F}^g = \sqrt{\vartheta^g} \mathbf{I} + [1 - \sqrt{\vartheta^g}] \mathbf{n}_0 \otimes \mathbf{n}_0$$

goriely, ben amar [2005], ben amar, goriely [2005,2007], socci, rennati, geraso, vena [2007], dervaux, ciarletta, ben amar [2009], goktepe, ablez, kuhl [2010], mc mahon, goriely [2010], buganza tepole, ploch, wong, gosain, kuhl [2011], buganza tepole, gosain, kuhl [2011], li, cao, feng, gao [2011]

example - skin expansion

37

time integration - euler backward



- finite difference approximation

$$\dot{\vartheta}^g = \frac{1}{\Delta t} [\vartheta^g - \vartheta_n^g] = k^g(\vartheta^g) \phi^g(\vartheta^e)$$

- residual of discrete evolution equation

$$\mathbf{R}^g = \vartheta^g - \vartheta_n^g - k^g \phi^g \Delta t \doteq 0$$

- linearized residual for local newton iteration

$$\mathbf{K}^g = \frac{\partial \mathbf{R}^g}{\partial \vartheta^g} = 1 - \left[\frac{\partial k^g}{\partial \vartheta^g} \phi^g + k^g \frac{\partial \phi^g}{\partial \vartheta^g} \right] \Delta t$$

- iterative update of growth multiplier

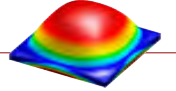
$$\vartheta^g \leftarrow \vartheta^g - \mathbf{R} / \mathbf{K}$$

the adrian me337-model [2010]

example - skin expansion

39

stretch-induced area growth



- growth tensor

$$\mathbf{F}^g = \sqrt{\vartheta^g} \mathbf{I} + [1 - \sqrt{\vartheta^g}] \mathbf{n}_0 \otimes \mathbf{n}_0$$

- area growth

$$\dot{\vartheta}^g = k^g(\vartheta^g) \phi^g(\vartheta^e)$$

- weighting function

$$k^g = [[\vartheta^{\max} - \vartheta^g] / [\vartheta^{\max} - 1]]^\gamma / \tau$$

- growth criterion

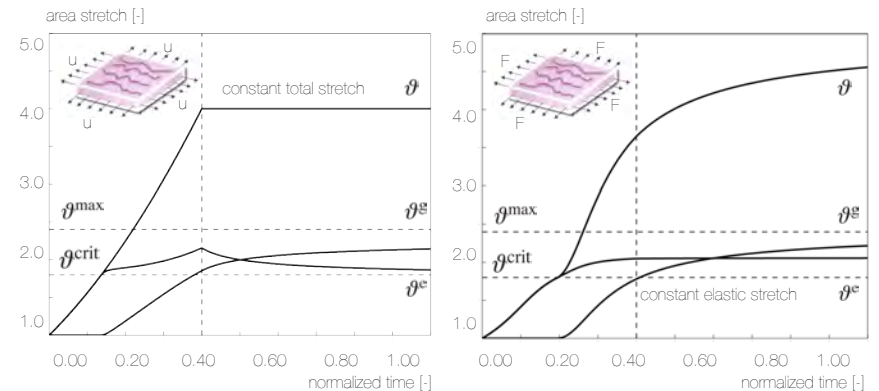
$$\phi^g = \vartheta^e - \vartheta^{\text{crit}} = \vartheta / \vartheta^g - \vartheta^{\text{crit}}$$

himpel, kuhl, menzel, steinmann [2005], kuhl, maas, himpel, menzel [2007], goktepe, ablez, parker, kuhl [2010], goktepe, ablez, kuhl [2010], schmid, pauli, paulus, kuhl [2011], buganza tepole, ploch, wong, gosain, kuhl [2011], buganza tepole, gosain, kuhl [2011]

example - skin expansion

38

relaxation & creep



temporal evolution of total area stretch, reversible elastic area stretch, and irreversible growth area stretch for displacement- and force-controlled skin expansion. displacement control induces relaxation, a decrease in elastic stretch, while the growth stretch increases at a constant total stretch. force control induces creep, a gradual increase in growth stretch and total stretch at constant elastic stretch.

example - skin expansion

40

current gold standard in expander selection



$$A_{\text{growth}} = A_t - A_0 = 2h [w+d]$$

empirical correction factors: 6.00, 3.75, and 4.50

van rappard, molenaar, van doom, sonneveld, borghouts [1988]
shively [1986], duits, molenaar, van rappard [1989]

example - skin expansion

41

predictive modeling for expander selection

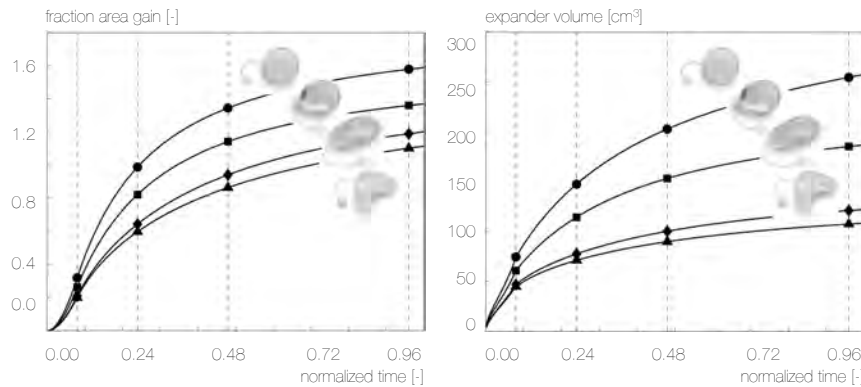


skin is modeled as a 0.2cm thin 1212cm² square sheet, discretized with 3'24'24=1728 trilinear brick elements, with 4'25'25=2500 nodes and 7500 degrees of freedom. the base surface area of all expanders is scaled to 148 elements corresponding to 37cm². this area, shown in red, is gradually pressurized from below while the bottom nodes of all remaining elements, shown in white, are fixed.

example - skin expansion

42

fractional area gain & expander volume



tissue expander inflation. expanders are inflated gradually between $t=0.00$ and $t=0.08$ by linearly increasing the pressure, which is then held constant from $t=0.08$ to $t=1.00$ to allow the skin to grow. under the same pressure, the circular expander displays the largest fractional area gain and expander volume, followed by the square, the rectangular, and the crescent-shaped expanders.

example - skin expansion

43

quantitative expander selection

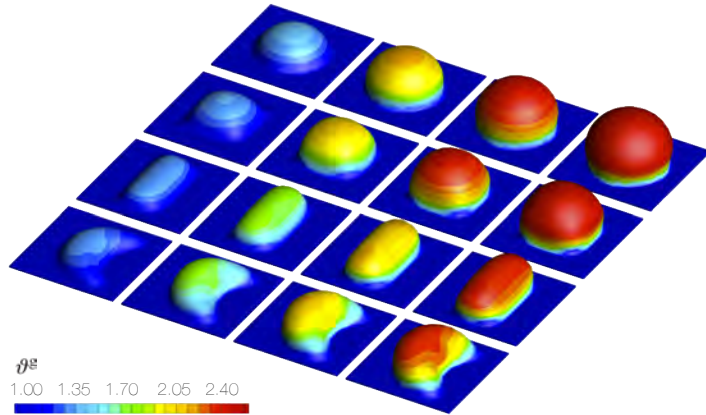
	maximum growth β^E [-]	initial area A_0 [cm ²]	absolute area gain ΔA [cm ²]	fractional area gain $\Delta A/A_0$ [-]	expander volume V [cm ³]	expander pressure p/E [-]	residual stress $(\sigma^{\text{max}})/E$ [-]
circular	2.36	37.00	58.74	1.59	257.45	0.002	0.42
square	2.35	37.00	50.63	1.37	186.77	0.002	0.41
rectangular	2.26	37.00	44.40	1.20	122.06	0.002	0.34
crescent	2.25	37.00	41.19	1.11	108.42	0.002	0.33

tissue expander inflation and deflation. maximum growth multiplier, absolute area gain, fractional area gain, and expander volume under constant pressure loading at time $t=50$ and maximum principal residual stresses upon unloading after a constant pressure growth until $t=12$ are largest for the circular expander, followed by the square, the rectangular, and the crescent shape expanders.

example - skin expansion

44

area growth - isotropic skin model

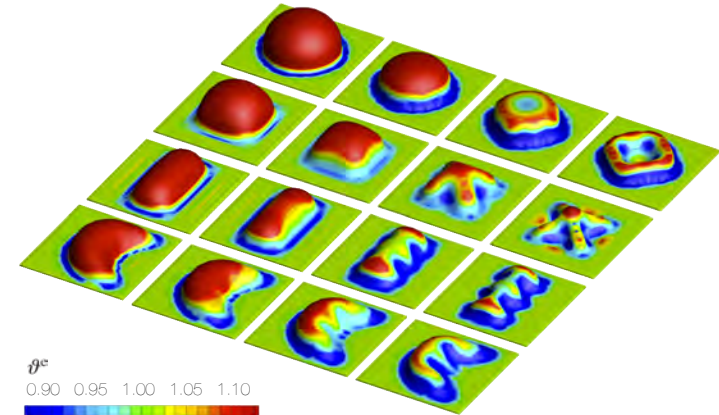


tissue expander inflation. spatio-temporal evolution of area growth. under the same pressure applied to the same base surface area, the circular expander induces the largest amount of growth followed by the square, the rectangular, and the crescent-shaped expanders.

example - skin expansion

45

elastic stretch - isotropic skin model

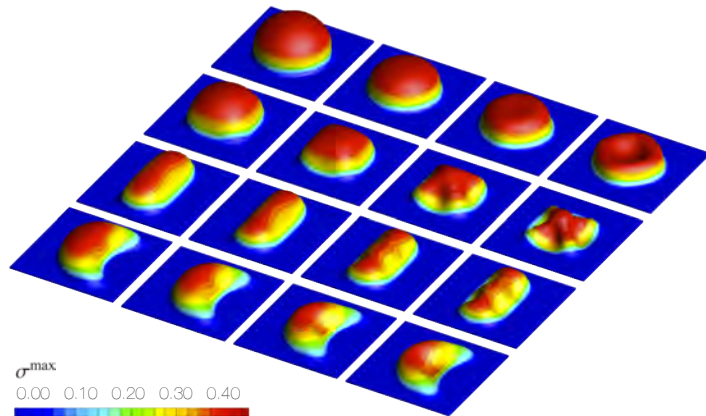


tissue expander deflation. spatio-temporal evolution of elastic area stretch. as the expander pressure is gradually removed, from left to right, the grown skin layer collapses. deviations from a flat surface after total unloading, right, demonstrate the irreversibility of the growth process.

example - skin expansion

46

residual stress - isotropic skin model



tissue expander deflation. spatio-temporal evolution of maximum principal stress. as the expander pressure is gradually removed, from left to right, the grown skin layer collapses. remaining stresses at in the unloaded state, right, are growth-induced residual stresses.

example - skin expansion

47

tissue expansion in pediatric forehead reconstruction

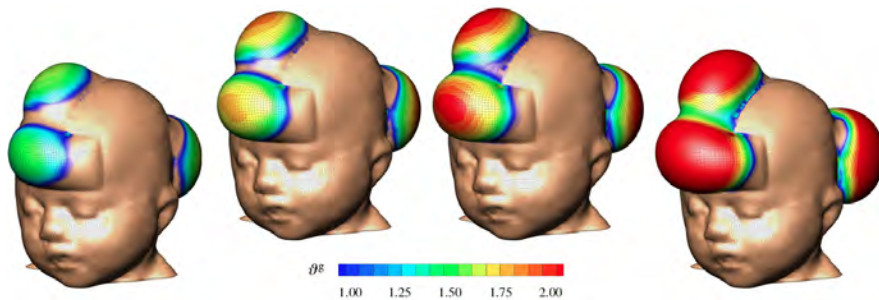


resurfacing of large congenital defects. the patient, a one-year old girl, presented with a giant congenital nevus. three forehead and scalp expanders were implanted simultaneously for in situ forehead flap growth. the follow-up photograph shows the girl at age three the initial defect was excised and resurfaced with expanded forehead and scalp flaps.

example - tissue expansion

48

tissue expansion in pediatric forehead reconstruction



skin expansion in pediatric forehead reconstruction. case study I: simultaneous forehead, anterior and posterior scalp expansion. spatio-temporal evolution of area growth displayed at $t=0.24$, $t=0.33$, $t=0.42$ and $t=0.75$. the initial area of 149.4cm^2 increases gradually as the grown skin area increases to 190.2cm^2 , 207.4cm^2 , 220.4cm^2 , and finally 251.2cm^2 , from left to right.

example - tissue expansion

49

tissue expansion in pediatric forehead reconstruction

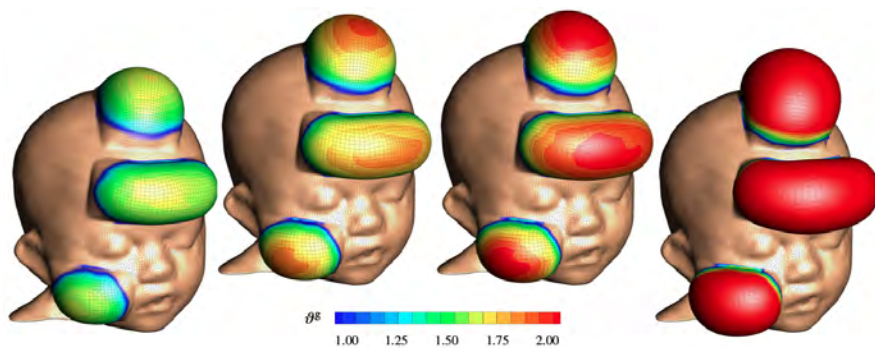


resurfacing of large congenital defects: the patient, a one-year boy, presented with a giant congenital nevus. simultaneous forehead, cheek, and scalp expanders were implanted for in situ skin growth. this technique allows to resurface large anatomical areas with skin of similar color, quality, and texture. the follow-up photograph shows the boy at age three after forehead reconstruction.

example - tissue expansion

50

tissue expansion in pediatric forehead reconstruction

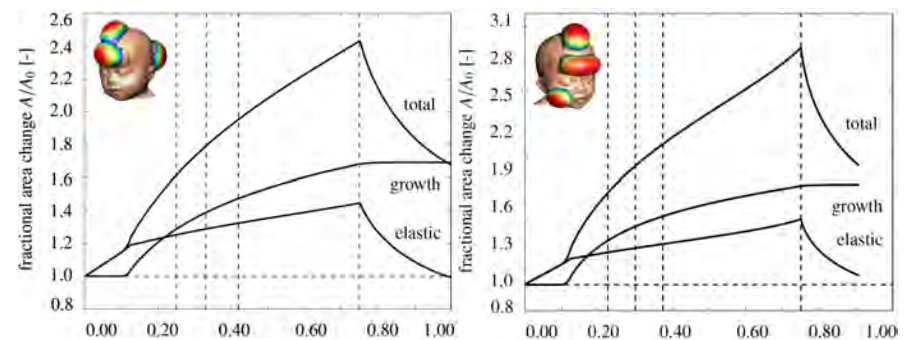


skin expansion in pediatric forehead reconstruction. case study II: simultaneous forehead, scalp, and cheek expansion. spatio-temporal evolution of area growth displayed at $t=0.24$, $t=0.33$, $t=0.42$ and $t=0.75$. the initial area of 128.7cm^2 increases gradually as the grown skin area increases to 176.0cm^2 , 191.3cm^2 , 202.1cm^2 , and finally 227.1cm^2 , from left to right.

example - tissue expansion

51

tissue expansion in pediatric forehead reconstruction



skin expansion in pediatric forehead reconstruction. case study I: simultaneous forehead, anterior and posterior scalp expansion, right. case study II: simultaneous forehead, scalp, and cheek expansion, left. vertical dashed lines correspond to the time points displayed in the previous figures.

example - tissue expansion

52